Monthly Notices
of the
ROYAL ASTRONOMICAL SOCIETY

Mon. Not. R. Astron. Soc. **425,** 34–43 (2012) doi:10.1111/j.1365-2966.2012.21367.x

ExoMol line lists – I. The rovibrational spectrum of BeH, MgH and CaH in the $X\,^2\Sigma^+$ state

Benjamin Yadin, Thomas Veness, Pierandrea Conti, Christian Hill,
Sergei N. Yurchenko and Jonathan Tennyson★

Department of Physics and Astronomy, University College London, Gower Street, WC1E 6BT London

Accepted 2012 May 16. Received 2012 May 16; in original form 2012 March 22

ABSTRACT

Accurate line lists for three molecules, BeH, MgH and CaH, in their ground electronic states are presented. These line lists are suitable for temperatures relevant to exoplanetary atmospheres and cool stars (up to 2000 K). A combination of empirical and ab initio methods is used. The rovibrational energy levels of BeH, MgH and CaH are computed using the programs LEVEL and DPOTFIT in conjunction with 'spectroscopic' potential energy curves (PECs). The PEC of BeH is taken from the literature, while the PECs of CaH and MgH are generated by fitting to the experimental transition energy levels. Both spin-rotation interactions (except for BeH, for which it is negligible) and non-adiabatic corrections are explicitly taken into account. Accurate line intensities are generated using newly computed ab initio dipole moment curves for each molecule using high levels of theory. Full line lists of rotation–vibration transitions for ^{9}BeH, ^{24}MgH, ^{25}MgH, ^{26}MgH and ^{40}CaH are made available in an electronic form as supporting information to this paper and at www.exomol.com.

Key words: molecular data – opacity – astronomical data bases: miscellaneous – planets and satellites: atmospheres – stars: low-mass.

1 INTRODUCTION

The ExoMol project aims to provide line lists of spectroscopic transitions for key molecular species which are likely to be important in the atmospheres of extrasolar planets and cool stars. The aims, scope and methodology of the project are summarized in the previous paper (Tennyson & Yurchenko 2012). In this paper, the first in a planned series, we present results for the electronic ground-state rotation–vibration spectra of three metal hydrides BeH, MgH and CaH, denoted generically as XH. The line lists are explicitly designed to extend to high temperatures. All three of these hydrides are of astronomical interest.

The alkaline earth metal species BeH, MgH and CaH share many similar properties. Early spectroscopic data on these three species are captured by Huber & Herzberg (1979). A summary of more recent studies, both spectroscopic and astrophysical, is presented for each molecule below.

1.1 BeH

BeH is one of the simplest heteronuclear diatomic molecules, and hence it is a strong contender for being observed in contexts such as exoplanetary atmospheres, cool stars and the interstellar medium. However, there are only very few astrophysical records of BeH, for example, a detection of $A\,^2\Sigma^+ \rightarrow X\,^2\Sigma^+$ emission lines of BeH in the sunspot umbra spectra by Wöhl (1971) and Shanmugavel et al. (2008).

BeH has been studied extensively by quantum chemists using different ab initio methods. It is the simplest open-shell molecule, which made it very popular as a benchmark object for testing new ab initio approaches. Ab initio studies on BeH are mostly limited by the basic spectroscopic and structural constants. Pitarch-Ruiz et al. (2008) reported very comprehensive electronic-structure calculations on BeH with the potential energy and dipole moments curves computed for a number of electronic states. A very accurate ab initio ground-state potential energy curve (PEC) was recently generated by Koput (2011). Le Roy et al. (2006) generated a 'spectroscopic' PEC of BeH obtained by fitting to the experimental values of Colin, Dreze & Steinhauer (1983), Focsa et al. (1998) and Shayesteh et al. (2003). This is currently the most accurate PEC of BeH, and we employ it here in our production of the line list for BeH.

★E-mail: j.tennyson@ucl.ac.uk

Experimental work on BeH is not so extensive: most of experimental studies of BeH have focused on electronic transitions (Degreef & Colin 1974; Colin et al. 1983; Clerbaux & Colin 1991; Focsa et al. 1998). Ground electronic state rotation–vibration spectra were reported by Shayesteh et al. (2003).

1.2 MgH

MgH is thought to be a likely candidate for interstellar observation but has yet to be detected (Sakamoto et al. 1998a). However, its presence in stellar spectra is well documented through observation of the $A\,^2\Pi \rightarrow X\,^2\Sigma^+$ (Sotirovski 1971) and $B'\,^2\Sigma^+ \rightarrow X\,^2\Sigma^+$ (Wallace et al. 1999) transitions. These transitions have been used as an indicator for the magnesium isotope abundances in the atmospheres of different stars (Lambert, Mallia & Petford 1971; Tomkin & Lambert 1980; Lambert & Mcwilliam 1986; Wallace et al. 1999; Gay & Lambert 2000; Yong, Lambert & Ivans 2003) from giants to dwarfs including the Sun. The same lines of MgH were used to measure the temperature of stars (e.g. Wyller 1961), surface gravity (e.g. Bell, Edvardsson & Gustafsson 1985; Bonnell & Bell 1993), stars' metal abundance (e.g. Cottrell 1978; Tomkin & Lambert 1980), gravitational acceleration (e.g. Berdyugina & Savanov 1992), to measure the temperature and pressure (Kulaczewski, Degenhardt & Kneer 1990), as well as for a deuterium test (Pavlenko et al. 2008). MgH is an important part of stellar atmospheric models, such as, for example, PHOENIX (Allard et al. 2001) which incorporates the MgH line list of Kurucz (2011).

MgH has been studied in laboratories since 1929 (see Pearse 1929), with measurements of rovibrational transitions in the $X\,^2\Sigma^+$ state given by Zink et al. (1990), Ziurys, Barclay & Anderson (1993) and most extensively by Shayesteh et al. (2004a). Many experimentally measured spectral lines exist for the $A\,^2\Pi \rightarrow X\,^2\Sigma^+$ and $B'\,^2\Sigma^+ \rightarrow X\,^2\Sigma^+$ transitions (Bernath, Black & Brault 1985; Shayesteh et al. 2007; Shayesteh & Bernath 2011), although the ground-state transitions have only been observed in the infrared (IR) up to $v = 4$. Experimental ground $X^2\Sigma^+$ state spectra were reported by Leopold et al. (1986), Lemoine et al. (1988), Zink et al. (1990) and Ziurys et al. (1993), which also include high-resolution millimetre-wave studies of the pure rotational transitions with the hyperfine structure resolved.

On the ab initio side, the calculations of the PECs and dipole moment curves (DMCs) of MgH by Saxon, Kirby & Liu (1978) made a very important contribution to the development of the theory for this molecule. The results of this study have been used in many spectroscopic applications including the ^{24}MgH line list from the UGAMOP (The University of Georgia Molecular Opacity Project) group (Weck et al. 2003a,b). Very recently, accurate ab initio calculations have been performed using significantly higher levels of theory (Mestdagh et al. 2009; Guitou, Spielfiedel & Feautrier 2010), with PECs and DMCs of MgH reported. Important theoretical work for this study is by Shayesteh et al. (2007), where an accurate 'spectroscopic' PEC of MgH was obtained by fitting to all existing experimental transitions for this molecule. We use this PEC as an initial approximation in our fits.

The first complete MgH line list was computed by Kurucz (see Kurucz 2011). This line list, however, overestimates the opacity of MgH when included into the atmospheric models due to presence of non-existent levels (see discussion by Weck et al. 2003b). Kurucz's line list does not include the ground rotation–vibration transitions and thus cannot be compared to the results of this work. The UGAMOP line lists (Weck et al. 2003a,b; Weck, Stancil & Kirby 2003c) mentioned above contain 23 315 transitions and associated oscillator strengths over the wavelength range 0–32 130 cm^{-1}, for all possible allowed transitions from the ground electronic state vibrational levels with $v'' \leq 11$.

1.3 CaH

The main astrophysical interest in CaH is because of the spectra of T Tauri stars (Di Rosa 2004). The transition lines of CaH were used in identifications and studies of different dwarfs (Barbuy et al. 1993; Reid et al. 1997; Burgasser et al. 2003; McGovern et al. 2004; Reiners et al. 2007), galactic discs (Reid et al. 1997), molecular clouds (Sakamoto et al. 1998b) and sunspots (Berdyugina et al. 2006). One of the most important spectroscopic features of the CaH spectra of T and L dwarfs is the 6750–7050 nm band covering the $A-X$ (0, 0) rotational transitions (Burgasser et al. 2003; Reiners et al. 2007).

CaH has been studied in the laboratory since Hulthèn (1927) and Watson & Weber (1935). Much experimental work has been done on the electronic transitions of CaH (Leininger & Jeung 1995; Weck, Stancil & Kirby 2003d; Chen et al. 2006; Ram et al. 2011), but only a few studies exist on the ground-state rovibrational spectrum. The most important experimental studies of CaH for the current work include the Fourier transform emission spectra of the $E\,^2\Pi-X\,^2\Sigma^+$ bands (Ram et al. 2011) and of four rovibrational bands in the $X\,^2\Sigma^+$ state of CaH and CaD (Shayesteh et al. 2004b). These works provided very accurate experimental measurements of rovibronic frequencies with a very thorough analysis. Other experimental work include spectra and analysis of the $A-X$ and $B-X$ systems of CaH and CaD (Berg & Klynning 1974; Berg, Klynning & Martin 1976; Klynning & Martin 1981; Martin 1984; Pereira et al. 2002; Gasmi et al. 2003); ultraviolet-absorption spectra of the *C*, *D*, *K*, *L*, *G*, *J* and *M* bands of CaH (Kaving & Lindgren 1974, 1976; Kaving, Lindgren & Ramsay 1974; Bell, Herman, Johns & Peck 1979; Kaving & Lindgren 1981); magnetic hyperfine structure of the $A-X$ and $B-X$ spectra of CaH (Steimle et al. 1987; Chen et al. 2006); and the IR (Petitprez et al. 1989; Frum & Pickett 1993) and millimetre-wave (Barclay, Anderson & Ziurys 1993; Frum et al. 1993) transitions within the ground electronic state.

From a very large number of ab initio studies of CaH we select here only the most recent and comprehensive works. The potential energy and DMCs of CaH were computed using different levels of theory (Boutalib, Daudey & Elmouhtadi 1992; Leininger & Jeung 1995; Holka & Urban 2006; Kerkines & Mavridis 2007). In most cases a number of equilibrium constants, including $r_{\rm e}$, $\omega_{\rm e}$ and $D_{\rm e}$, as well as the permanent dipole moments μ_e were reported for one or several low-lying states. To our knowledge there are no experimental absolute intensity measurements of CaH. However, a few lifetime measurements for a number of low-lying vibrational states $v = 0$, 1, 2 of the *X*, *A* and *B* states were used to estimate the corresponding oscillator strengths or Einstein coefficients (Klynning et al. 1982; Berg, Ekvall & Kelly 1996; Liu et al. 2009). The permanent electric dipole moments of CaH were obtained experimentally for a few low electronic states using the Stark effect (Steimle, Chen & Gengler 2004; Chen & Steimle 2008).

As far as the theoretical rovibronic studies on CaH are concerned, there have been attempts to refine PECs by fitting to available experimental energies or frequencies (Martin 1988; Uehara 1998; Urena et al. 2000). However, previous rovibronic models did not include a proper description of different important couplings between electronic states. Therefore, only the ground electronic state could be reasonably well described in this approach, for example, by Uehara (1998) who also included the Born–Oppenheimer breakdown

(BOB) effect. None of these studies take account of spin-rotational splittings. Carlsund-Levin et al. (2002) presented an accurate model with an explicit coupling of four lowest electronic states as well as the BOB effect using previously published ab initio PECs by Martin (1988). However, since these PECs are of ab initio (not experimental) accuracy, the resulting energies were only good enough to validate the models used, but not to predict the corresponding frequencies of CaH and CaD.

The most comprehensive line list for ^{40}CaH was reported by Weck et al. (2003d), who produced a complete list of CaH rovibrational levels and oscillator strength covering all possible allowed and bound transitions (89 970) in the frequency range up to 35 000 cm^{-1} involving the $X\,^2\Sigma^+$, $A\,^2\Pi$, $B/B'\,^2\Sigma^+$, $C\,^2\Sigma^+$, $D\,^2\Sigma^+$ and $E\,^2\Pi$ states. This line list should be good up to at least 2000 K and is also included into the UGAMOP data base. In the production of these data the authors used the most recent set of theoretical PECs and DMCs, with adjustments to account for experimental dissociation energies and asymptotic limits. However, the model used to compute the frequencies was not very accurate: (i) no fine structure, such as spin rotation, or non-adiabatic effects were taken into account and (ii) the PECs were not adjusted to the experiment; thus, the overall accuracy is no better than 10 to 30 cm^{-1}.

In this work, we present detailed line lists for BeH, ^{24}MgH, ^{25}MgH, ^{26}MgH and ^{40}CaH considering only the rotation–vibration transitions in the $X\,^2\Sigma^+$ state. At temperatures up to about 2000 K, any population of excited electronic states will be insignificant compared to the population of the ground state. Taking typical values for energies in the ground and first excited states of XH (Kerkines & Mavridis 2007; Pitarch-Ruiz et al. 2008; Guitou et al. 2010), the thermalized, relative population of the lowest rovibrational level of the first excited electronic state to that of the ground state for BeH, MgH and CaH can be estimated to be 2×10^{-6}, 2×10^{-5} and 1×10^{-4}, respectively, at 2000 K. In practice, the excited states are all close to or above the dissociation limits for the species so dissociative processes will further deplete the excited-state populations.

2 METHOD

For the species XH we solve the Schrödinger equation allowing for BOB effects as given by Shayesteh et al. (2007) using two programs, LEVEL 8.0 (Le Roy 2007) and DPOTFIT 1.1 (Le Roy 2006).

We did not generate new ab initio PECs for BeH and MgH. Full sets of potential parameters representing very accurate PECs for these molecules were already available from Le Roy et al. (2006) and Shayesteh et al. (2007), respectively. Ab initio PECs for CaH were generated using multiple levels of theory, beginning with a simple Hartree–Fock method and progressing to complete active space self-consistent field and multireference configuration interaction (MRCI; Knowles & Werner 1988). The best potential, with no unphysical kinks and a shape in agreement with previous works (Shayesteh et al. 2004b; Kerkines & Mavridis 2007), used the MRCI/aug-cc-pV5Z level of theory. All electronic structure calculations were performed with the quantum chemistry package MOLPRO 2010 (Werner et al. 2010). The PECs of BeH, MgH, and CaH are shown in Fig. 1.

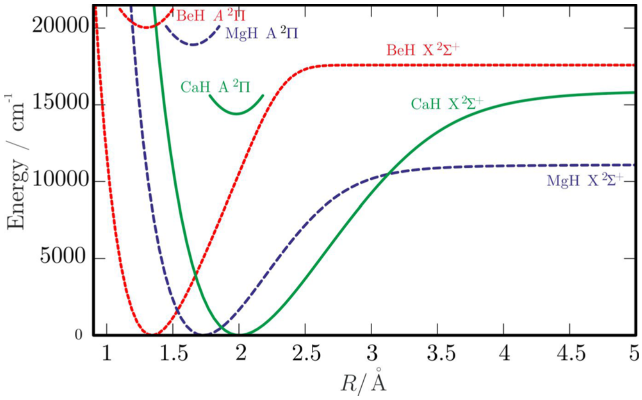

Figure 1. PECs of CaH (solid line), MgH (dashed line) and BeH (dotted line) in their ground electronic states. The associated first excited states are also indicated.

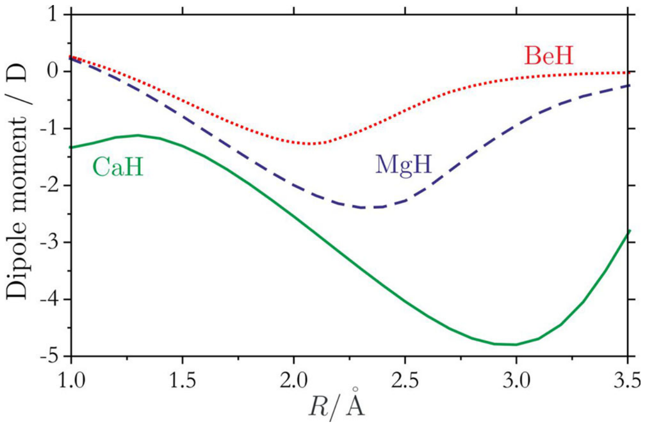

Figure 2. The ab initio DMCs of BeH, MgH and CaH in their ground electronic states selected for the line list production.

The DMCs for all three molecules were generated ab initio employing MOLPRO and different levels of theory. The best DMCs for each molecule (shown in Fig. 2) were selected based on their smoothness and agreement with published curves (Saxon et al. 1978; Leininger & Jeung 1995; Pitarch-Ruiz et al. 2008; Guitou et al. 2010). The DMCs were calculated using a finite field rather than as an expectation value as this is known to give more accurate results (Lodi & Tennyson 2010).

For BeH the final DMC was computed using the aug-cc-pwCV5Z basis set and the MRCI method on a grid of 45 geometries distributed between 1.3 and 10 Å. Our equilibrium dipole moment is −0.224 D at $r_e = 1.342$ Å. This can be compared to −0.199 D (Pitarch-Ruiz et al. 2008) for the same value of r_e.

For MgH the final DMC was calculated using RCCSD(T) [Restricted Coupled Cluster Single Doubles (with pertubative Triples)] (Knowles, Hampel & Werner 1993, 2000) in conjunction with the basis sets cc-pCV5Z (Woon & Dunning 1995) for Mg and aug-cc-pV5Z (Woon & Dunning 1993) for H and all electrons correlated. The good performance of the Restricted Hartree–Fock CCSD methods in the case of MgH was noted by Li & Paldus (1995). At r_e = 1.730 Å we obtain an equilibrium value of the dipole moment μ_e of −1.371 D. This can be compared to the CCSD(T) value from Serrano & Canuto (1998), −1.356 D. Our DMC agrees surprisingly well with dipole curves computed ab initio by Saxon et al. (1978).

The DMC for CaH was also calculated using RCCSD(T)/cc-pCV5Z with all electrons correlated. Holka & Urban (2006) demonstrated the importance of the electron correlation contribution (0.44 D or 17.4 per cent of the total value), while the relativistic and complete basis set corrections are relatively small (about 0.009 and 0.007 D, respectively). Our equilibrium value of the RCCSD(T)/cc-pCV5Z dipole moment is 2.55 D, which can be compared to the experimentally derived value of the permanent dipole moment 2.53(3)

D measured for the ground $X\,^2\Sigma^+(v=0)$ state with the optical Stark effect (Chen & Steimle 2008). Holka & Urban (2006) recently obtained an ab initio value of 2.463 D for μ_e using a high level of theory.

In all our calculations the ab initio DMC grid points were used directly in LEVEL.

2.1 Fitting the potential

In the case of BeH we employed the spectroscopic PEC of Le Roy et al. (2006) consisting of an extended Morse oscillator function corrected by the BOB effect. We could not precisely reproduce the rovibrational energies reported in this paper using these potential parameters and LEVEL 8.0, see columns II and III of Table 1. The deviations in the vibrational term values are rather small, except for $v = 11$ which is about 10 cm^{-1}; therefore, we decided to employ the PEC from Le Roy et al. (2006) in the line list calculations without any additional refinements.

In the case of the PEC of MgH we experienced a similar problem. Using the potential parameters from Shayesteh et al. (2007) in conjunction with the Morse long range (MLR) potential (Le Roy & Henderson 2007) in the DPOTFIT calculations we could not reproduce frequencies obtained by Shayesteh et al. (2007) using the same program. Considering the importance of MgH for astrophysical applications we decided to refine the Shayesteh et al. (2007) parameters through fits to the experimental data and using the same program (i.e. DPOTFIT 1.1) to guarantee the quality of the line list produced. In these fits, to avoid dealing with the high electronic states, we constructed a set of 'fake' transitions within the ground electronic states from the experimental transitions $A\,^2\Pi \rightarrow X\,^2\Sigma^+$ and $B\,^2\Sigma^+ \rightarrow X\,^2\Sigma^+$ using the method of the combination differences. As a result our 'experimental' set included 1302 transition frequencies, 380 of which were actual experimental, while the rest were 'experimentally' derived values. Some of the lines, especially from highly excited vibrational excitations, had a greater uncertainty and therefore were given a lower weighting. Despite their relatively low quality, these data are important to fix the behaviour of the potential at large intermolecular distances and hence to accurately predict the higher energy states. The fit was found to be unstable unless the dissociation energy D_e was held fixed – the best available value of 11 104.7 cm^{-1} from Shayesteh et al. (2007) was chosen.

Table 1. A comparison of the theoretical and experimental spectroscopic constants of BeH in cm^{-1}.

	Obs.[a]	Calc.[b]	Obs.−Calc.	Le Roy et al. (2006)
T_1	1986.4442	1986.4176	0.0266	1986.4163
T_2	3896.8785	3896.8714	0.0071	3896.8712
T_3	5729.2861	5729.2618	0.0243	5729.2602
T_4	7480.4528	7480.3400	0.1128	7480.3383
T_5	9145.2834	9145.2533	0.0301	9145.1320
T_6	10 716.2804	10 716.6292	−0.3488	10 716.1629
T_7	12 182.323	12 183.0505	−0.7275	12 182.2070
T_8	13 525.889	13 526.6563	−0.7673	13 525.7882
T_9	14 717.860	14 718.8262	−0.9662	14 718.0819
T_{10}	15 709.040	15 710.4672	−1.4272	15 709.3839
T_{11}	–	16 402.0939	–	16 412.7734
B_0	10.164 8880	10.165 644	-7.56×10^{-4}	10.165 715
B_1	9.855 4335	9.855 734	-3.01×10^{-4}	9.855 827
B_2	9.541 7271	9.541 630	0.98×10^{-4}	9.541 718
B_3	9.220 768	9.220 113	6.55×10^{-4}	9.220 280
B_4	8.886 639	8.886 566	0.73×10^{-4}	8.886 738
B_5	8.533 209	8.534 221	-10.12×10^{-4}	8.534 429
B_6	8.152 609	8.152 146	4.63×10^{-4}	8.153 772
B_7	7.729 457	7.722 324	71.33×10^{-4}	7.728 265
B_8	7.2309	7.214 164	166.86×10^{-4}	7.225 306
B_9	6.5921	6.570 639	214.91×10^{-4}	6.579 663
B_{10}	5.6984	5.662 832	355.38×10^{-4}	5.667 413
B_{11}	–	–		4.268 157

[a] Experimentally derived by Focsa et al. (1998).
[b] Calculated, this work.

Table 2. A comparison of the theoretical and experimental spectroscopic constants of ^{24}MgH in cm^{-1}.

	Obs.[a]	Calc.[b]	Obs.−Calc.	UGAMOP
T_1	1431.977 86	1431.9777	0.0002	1423.0023
T_2	2800.678 07	2800.6770	0.0011	2784.3944
T_3	4102.329 75	4102.3281	0.0017	4081.3781
T_4	5331.3892	5331.3867	0.0025	5308.9675
T_5	6479.6562	6479.6547	0.0015	6459.3356
T_6	7534.8137	7534.8076	0.0061	7521.0069
T_7	8477.9997	8477.9959	0.0038	8477.2820
T_8	9279.6527	9279.6436	0.0091	9299.8872
T_9	9892.7243	9892.7201	0.0042	9929.2662
T_{10}	10 249.4074	10 249.4050	0.0020	10 150.2699
T_{11}	10 352.25	10 352.2503	0.00	10 231.8603
B_0	5.736 507 68	5.736 5078	-0.01×10^{-5}	–
B_1	5.555 288 01	5.555 288 04	-0.003×10^{-5}	–
B_2	5.367 512	5.367 563 16	-5.12×10^{-5}	–
B_3	5.169 725	5.169 814 89	-8.99×10^{-5}	–
B_4	4.956 539	4.956 676 78	-13.78×10^{-5}	–
B_5	4.719 38	4.719 710 01	-33.00×10^{-5}	–
B_6	4.444 31	4.444 738 68	-42.87×10^{-5}	–
B_7	4.1072	4.106 958 83	24.12×10^{-5}	–
B_8	3.658 77	3.659 719 97	-95.00×10^{-5}	–
B_9	3.007 81	3.007 472 54	33.75×10^{-5}	–
B_{10}	1.9687	1.968 4569	24.31×10^{-5}	–
B_{11}	0.884	0.886 890 93	-289.09×10^{-5}	–

[a] Experimentally derived by Shayesteh et al. (2007).
[b] Calculated, this work.

The fit of the MgH potential achieved a root-mean-square (rms) error of 0.0012 cm^{-1} for the 380 experimental $X\,^2\Sigma^+ – X\,^2\Sigma^+$ lines with a maximum difference of 0.0077 cm^{-1}, showing that these lines are reproduced to high accuracy despite the inclusion of extra lines in the fit. Compared with the experimental line list (6076 lines) calculated by combination differences, the rms error is 0.059 cm^{-1} and the maximum difference is 0.35 cm^{-1}. The 'experimentally' derived lines show an inherent uncertainty of up to about 0.2 cm^{-1}.

To our knowledge there is no potential for CaH in the literature of a satisfactory accuracy. Therefore, we built a new 'spectroscopic' PEC for this molecule using the MLR potential. Fitting to the experimental data requires a good initial estimate for the PEC, for which our MRCI-Q/aug-cc-pV5Z potential was used. The corresponding MLR potential parameters were obtained through a fitting to the ab initio energies (see above) distributed over the geometry range from 0.7 to 10.0 Å. The potential was then refined by fitting to a list of 426 transition frequencies of ^{40}CaH by Shayesteh et al. (2004b) and Ram et al. (2011). We obtained higher accuracy fits if D_e was allowed to vary. Our value of $D_e = 15\,923$ cm^{-1} ended up somewhat higher than the experimental value 14 800 cm^{-1} (Huber & Herzberg 1979). The CaH fit achieved an rms of 0.001 cm^{-1} for 426 lines, the most complete data set we could build for fitting against. It should also be noted that no differences exceeded 0.0087 cm^{-1}.

Table 3. A comparison of the theoretical and experimental spectroscopic constants of ^{40}CaH in cm^{-1}.

	Obs.[a]	Calc.[b]	Obs.−Calc.	UGAMOP
T_1	1260.12775	1260.1275	0.0003	1248.1020
T_2	2481.99888	2481.9986	0.0003	2459.1800
T_3	3665.4141	3665.4135	0.0006	3634.0060
T_4	4809.9464	4809.9453	0.0011	4772.1695
T_5	–	5914.8483	–	5873.3462
T_6	–	6979.2865	–	6936.7620
T_7	–	8002.3180	–	7957.0594
T_8	–	8982.6564	–	8926.4122
T_9	–	9918.3259	–	9836.9332
T_{10}	–	10806.3117	–	10680.8451
T_{11}	–	11642.2418	–	11447.2650
T_{12}	–	12420.0739	–	12118.8518
T_{13}	–	13131.7349	–	12676.5357
T_{14}	–	13766.6602	–	13121.7989
T_{15}	–	14311.2476	–	13461.1465
T_{16}	–	14748.4857	–	13696.1992
T_{17}	–	15059.0529	–	
B_0	4.2286902	4.22868360	0.66×10^{-5}	–
B_1	4.131722	4.13171966	0.23×10^{-5}	–
B_2	4.0342454	4.03424554	-0.01×10^{-5}	–
B_3	3.935887	3.93589433	-0.73×10^{-5}	–
B_4	3.836122	3.83614878	-2.68×10^{-5}	–
B_5	–	3.73452399	–	–
B_6	–	3.63062100	–	–
B_7	–	3.52382050	–	–
B_8	–	3.41293766	–	–
B_9	–	3.29601845	–	–
B_{10}	–	3.17024576	–	–
B_{11}	–	3.03183969	–	–
B_{12}	–	2.87582915	–	–
B_{13}	–	2.69557438	–	–
B_{14}	–	2.48189083	–	–
B_{15}	–	2.22158167	–	–
B_{16}	–	1.89536199	–	–
B_{17}	–	1.47691639	–	–

[a] Experimentally derived by Shayesteh et al. (2004b).
[b] Calculated, this work.

Table 4. The completeness and coverage of our line lists for BeH, MgH and CaH.

	^{9}BeH	^{24}MgH	^{25}MgH	^{26}MgH	^{40}CaH
$\nu_{\max}$ (cm^{-1})	16 400	10 354	10 354	10 355	15 278
$v_{\max}$	11	11	11	11	19
$N_{\max}$	59	60	60	61	74
N_{lines}	3968	6716	6751	6754	26 980

For CaH, the most important change from the initial ab initio parameters is attributed to the equilibrium geometry. The initial parameters of MgH, being already empirical, however, were significantly less affected by the fitting process.

To illustrate the quality of these PECs, Tables 1–3 compare our vibrational energies, T_v, and rotational constants, B_v, with the corresponding ‘experimental’ (when available) and other theoretical values. In the case of MgH and CaH we list the UGAMOP theoretical values (Skory et al. 2003; Weck et al. 2003a,b,c,d), while for BeH ab initio spectroscopic constants of Le Roy et al. (2006) are given. When comparing to our energies it should be remembered that the UGAMOP energies do not include the spin-rotational splitting. Our results exhibit a significant improvement relative to the UGAMOP values for MgH and CaH.

Table 5. Extracts from the line list files for MgH, CaH and BeH.

$\tilde{\nu}_{ij}$	A_{ij}	$\tilde{E}''$	N'	p'	v'	N''	p''	v''
		^{24}MgH						
91.048 711	2.142 280E-01	320.031 578	8	*f*	0	7	*f*	0
91.073 979	2.430 318E-01	320.227 037	8	*e*	0	7	*e*	0
91.972 295	3.231 341E-01	4472.543 625	9	*f*	3	8	*f*	3
91.993 639	3.614 000E-01	4472.733 852	9	*e*	3	8	*e*	3
92.716 937	3.674 842E-01	6900.960 666	10	*f*	5	9	*f*	5
92.734 931	4.063 714E-01	6901.144 783	10	*e*	5	9	*e*	5
92.839 961	1.965 889E-01	9918.094 815	14	*f*	8	13	*f*	8
92.846 033	2.111 897E-01	9918.247 096	14	*e*	8	13	*e*	8
92.884 148	3.860 760E-03	10 261.123 179	1	*e*	11	2	*e*	10
92.893 287	2.144 867E-03	10 261.112 833	1	*f*	11	2	*f*	10
		^{40}CaH						
15.718 268	3.013 840E-03	3673.267 366	2	*f*	3	1	*f*	3
15.757 038	5.424 912E-03	3673.325 586	2	*e*	3	1	*e*	3
16.110 939	2.957 107E-03	2490.047 709	2	*f*	2	1	*f*	2
16.132 829	6.775 908E-03	13 147.887 247	3	*f*	13	2	*f*	13
16.151 200	5.322 792E-03	2490.108 168	2	*e*	2	1	*e*	2
16.154 575	6.453 246E-03	13 147.941 920	3	*e*	13	2	*e*	13
16.500 092	2.878 773E-03	1268.370 045	2	*f*	1	1	*f*	1
16.541 842	5.181 792E-03	1268.432 737	2	*e*	1	1	*e*	1
16.887 199	2.782 460E-03	8.434 990	2	*f*	0	1	*f*	0
16.930 436	5.008 428E-03	8.499 915	2	*e*	0	1	*e*	0
		^{9}BeH						
19.079 220	1.306 725E-04	3896.871 469	1		2	0		2
19.707 403	9.607 023E-05	1986.417 648	1		1	0		1
20.327 181	6.337 485E-05	0.000 000	1		0	0		0
22.576 116	6.097 568E-04	15 721.783 485	2		10	1		10
23.667 196	2.713 953E-04	16 426.182 379	3		11	2		11
26.231 114	1.246 778E-03	14 731.961 064	2		9	1		9
28.814 926	1.753 481E-03	13 541.079 476	2		8	1		8
30.852 363	2.056 734E-03	12 198.490 607	2		7	1		7
30.856 982	5.807 508E-04	16 449.849 576	4		11	3		11
32.574 171	2.147 658E-03	10 732.929 225	2		6	1		6

$\tilde{\nu}_{ij}$: transition frequency in cm^{-1}; A_{ij}: Einstein *A*-coefficient in s^{-1}; $\tilde{E}''$: lower state energy in cm^{-1}; N': upper state rotational quantum number; p': upper state rotationless parity; v': upper state vibrational quantum number; N'': lower state rotational quantum number;p'': lower state rotationless parity; v'': lower state vibrational quantum number.

3 LINE LIST CALCULATIONS

The procedure described above was used to produce line lists for the XH species, i.e. catalogues of transition frequencies $\tilde{\nu}_{ij}$ and Einstein coefficients A_{ij}. The computed line lists for BeH, ^{24}MgH, ^{25}MgH, ^{26}MgH and ^{40}CaH are given in the supporting information with the electronic version of this paper. The same ‘spectroscopic’ PEC of MgH corrected for BOB was used to produce the line lists for all three isotopologues of this species. The coverage in terms of the frequency range and quantum numbers is illustrated in Table 4.

The line list file, see Table 5, contains transition frequencies $\tilde{\nu}_{ij}$ (cm^{-1}), Einstein coefficients A_{ij} (s^{-1}), lower (i) state term values $\tilde{E}_i''$ (cm^{-1}) and upper and lower state quantum numbers for each line. Quantum numbers are defined in accordance with Hund’s case (b) formulation: N specifies the total angular momentum excluding spin, $J = N \pm 1/2$ specifies the total angular momentum including electron spin and *e*/*f* is the rotationless parity: the sign of the total parity is defined by $(-1)^N$ for a Σ^+ electronic state so states with

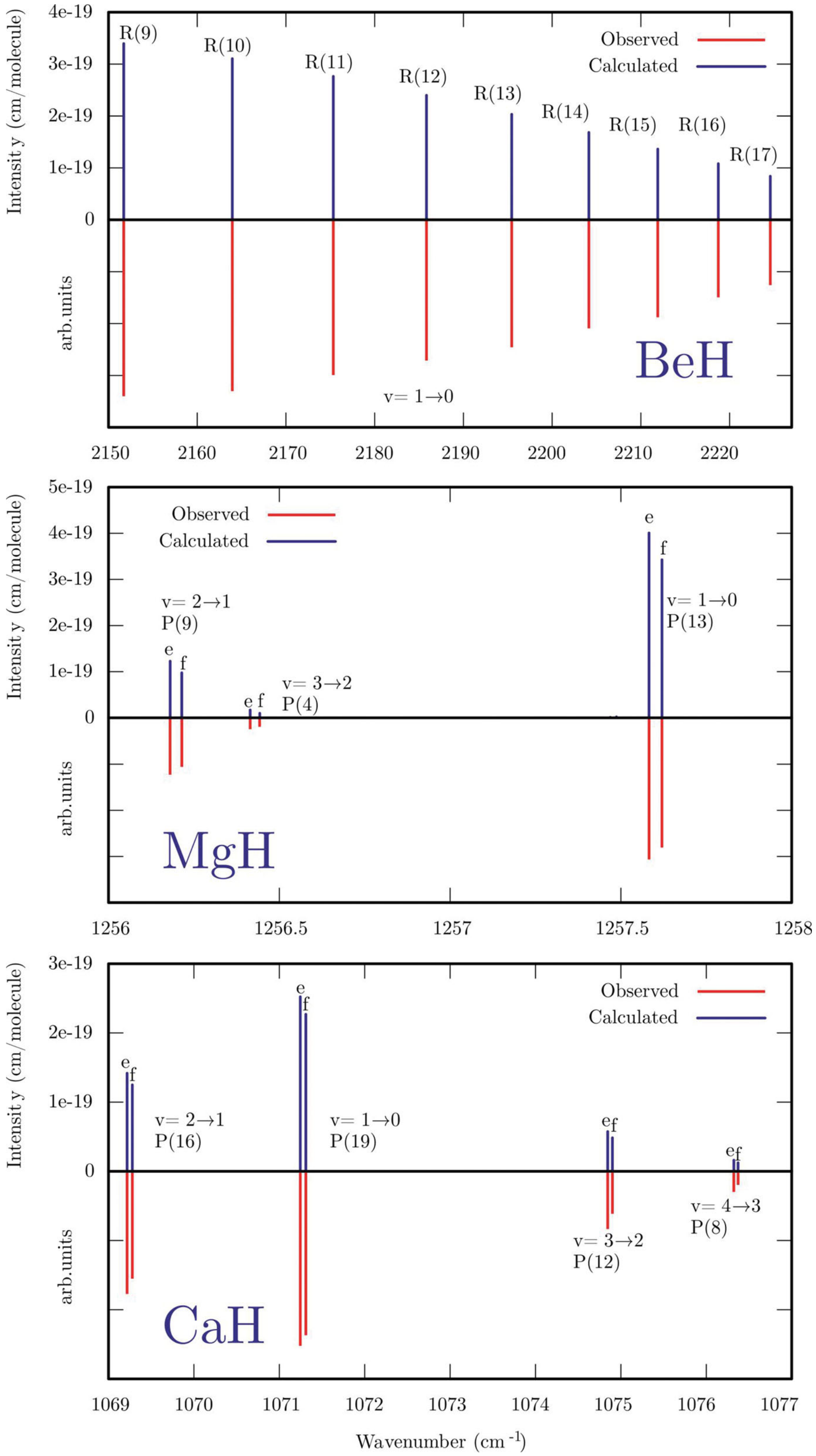

Figure 3. Theoretical stick absorption spectra of BeH, ^{24}MgH and ^{40}CaH at the room temperature compared to the experimental data reported by Shayesteh et al. (2003), Shayesteh et al. (2004a) and Shayesteh et al. (2004b), respectively. The experimental spectra are scaled to match the theoretical intensities.

$J = N + 1/2$ are e states and those with $J = N - 1/2$ are f states (Brown et al. 1975); and the vibrational quantum number v. Since we ignore hyperfine effects due to the interaction with the nuclear spins, J is assumed to be a conserved quantity. The *e*/*f* labels are omitted from the BeH line list as we consider the corresponding energies to be degenerate. The energy levels are given relative to the corresponding zero-point energy $E^e_{N=0,v=0}$.

The spin-rotational coupling plays an important role in the case of rovibrational spectra of both MgH and CaH, in contrast to BeH, where the fine structure can be considered negligible. The program LEVEL is not capable of treating the spin-rotation coupling, and therefore the corresponding rovibrational energies of MgH and CaH were computed with the program DPOTFIT. Only the Einstein coefficients were generated using LEVEL, i.e. without spin-rotation effects included. We assume that the *e*–*f* intensities are negligible, while the transition moments for *e*–*e* and *f*–*f* transitions are equal (see also discussion in the book by Herzberg 1989). This can be readily verified for MgH: the known experimental *e*–*f* transitions are indeed very weak (Shayesteh et al. 2004a), and for CaH no such transitions were reported experimentally, probably for the same reason. It should be noted that the LEVEL program computes the line strengths as 'singlet–singlet' transitions and the following correction factors had to be applied (Watson 2008) in order to account for the fine structure in the MgH and CaH transitions:

$$S^R(f \rightarrow f) = S^R_{\rm Level}\frac{2J''+1}{2J''+2}, \tag{1}$$

$$S^P(f \rightarrow f) = S^P_{\rm Level}\frac{2J''-1}{2J''}, \tag{2}$$

$$S^R(e \rightarrow e) = S^R_{\rm Level}\frac{2J''+3}{2J''+2}, \tag{3}$$

$$S^P(e \rightarrow e) = S^P_{\rm Level}\frac{2J''+1}{2J''}. \tag{4}$$

Here $S^{R/P}$ is the line strength of the *R*/*P* transition.

The integrated absorption coefficient $I(\omega_{ij})$ for an $i \rightarrow j$ transition can be calculated for a specific temperature T using

$$I(\omega_{ij}) = \frac{\alpha A_{ij} g_j}{Z(T)\omega_{ij}^2}\left(\mathrm{e}^{-E''/k_{\rm B}T} - \mathrm{e}^{-E'/k_{\rm B}T}\right), \tag{5}$$

where g_j is the degeneracy of the final state, $Z(T)$ is the partition function, $k_{\rm B}$ is the Boltzmann constant, E' is the energy of the higher state, E'' is the energy of the lower state, ω (cm^{-1}) is the transition wavenumber and α is the factor $1.327\,1005 \times 10^{-12}$ s cm^{-2} molecule^{-1} so that I has units of cm molecule^{-1}. For the $X\,^2\Sigma$ state of BeH, where the states i are doubly degenerate, the partition function, $Z(T)$, is given by

$$Z(T) = \sum_i g_i \mathrm{e}^{-E_i/k_{\rm B}T} = \sum_i g_{\rm ns}(2S+1)(2N_i+1)\mathrm{e}^{-E_i/k_{\rm B}T}, \tag{6}$$

where $S = 1/2$ is the total electronic spin angular momentum, $g_{\rm ns} = 8$ is the nuclear statistical weight of BeH and N_i is the rotational angular momentum of the nuclei of the ith state. Here, we follow the HITRAN (Simeckova et al. 2006) convention and consider the nuclear statistical weight of the molecule explicitly in $Z(T)$. In the case of MgH and CaH in their ground electronic states the spin-rotational splitting is resolved and $Z(T)$ is given by

$$Z(T) = \sum_i g_{\rm ns}(2J_i+1)\mathrm{e}^{-E_i/k_{\rm B}T}. \tag{7}$$

Here, the nuclear statistical weights $g_{\rm ns} = 2$ for ^{40}CaH, ^{24}MgH and ^{26}MgH, and $g_{\rm ns} = 12$ for ^{25}MgH. The nuclear spins of ^{25}Mg and Be used to define these values are 5/2 and 3/2, respectively, whilst the nuclear spins of ^{24}Mg, ^{26}Mg and ^{40}Ca are 0.

High-resolution comparisons with specific regions of the experimental spectra for each molecule are given in Fig. 3; note that the experimental spectrum has been scaled to the theoretical data by matching one line since none of the reported measurements are absolute. These comparisons demonstrate the accuracy of our procedure. In Figs 4–6 we also compare synthetic absorption spectra of CaH and MgH at the room temperature as well as at $T = 1500$ K generated using our and the UGAMOP line lists. The line intensities in these figures are given by sticks. For a better comparison the UGAMOP line intensities are divided by 2 in order to account for the difference in treating the fine (i.e. spin-rotational) splitting. In the case of CaH our intensities in the higher frequency range are systematically weaker than that of UGAMOP. Fig. 7 illustrates a 1500 K absorption spectrum for BeH.

3.1 Partition function

We used the calculated energies of all three molecules to generate the partition function values for a range of temperatures from 0 to 3000 K. These values were represented by the following polynomial expansion (Vidler & Tennyson 2000) via a least-squares fit:

$$\log(Z) = \sum_{n=1}^{6} a_i \log(T)^i. \tag{8}$$

The resulting expansion constants a_i for BeH, ^{24}MgH and ^{40}CaH are listed in Table 6. To a very good approximation the partition functions of ^{24}MgH, ^{25}MgH and ^{26}MgH are in the ratio 2:12:2, which takes account of the increased nuclear spin statistical weight of ^{25}MgH. This scaling can be used to obtain $Z(T)$ for the latter two species.

We have also compared our $Z(T)$ of CaH to the partition function values computed using the UGAMOP energies of CaH. Even though the difference between our and UGAMOP energies is large (Table 3), the partition functions agree within 3 per cent for the whole range of T up to 3000 K.

Irwin (1981) and Sauval & Tatum (1984) reported similar expansions of $Z(T)$ for a large set of molecules, which we can use to validate our results. For example, for ^{24}MgH at $T = 2000$ K from

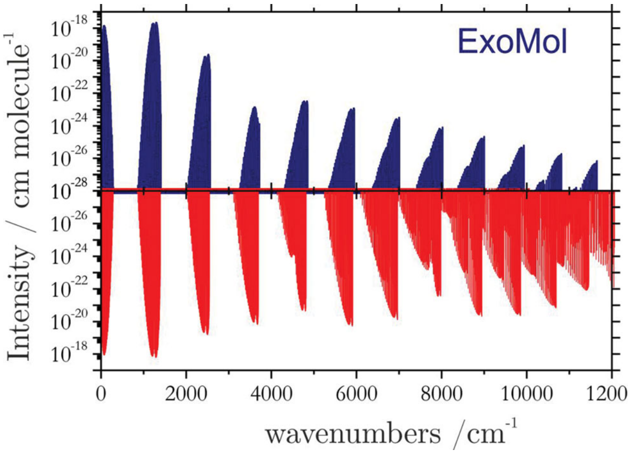

Figure 4. Absorption spectra of CaH at $T = 296$ K: ExoMol versus UGAMOP.

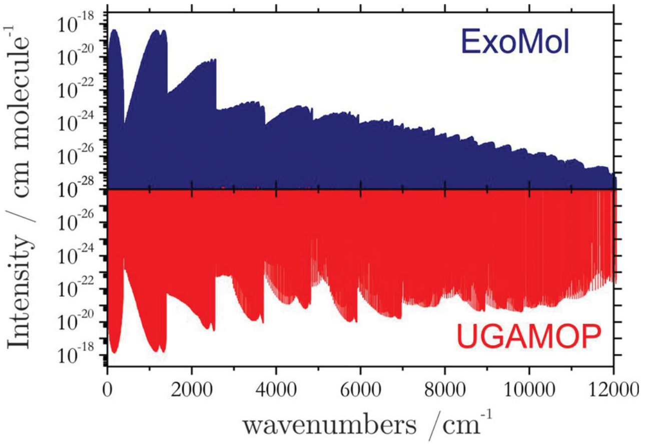

Figure 5. Absorption spectra of CaH at T = 1500 K: ExoMol versus UGAMOP.

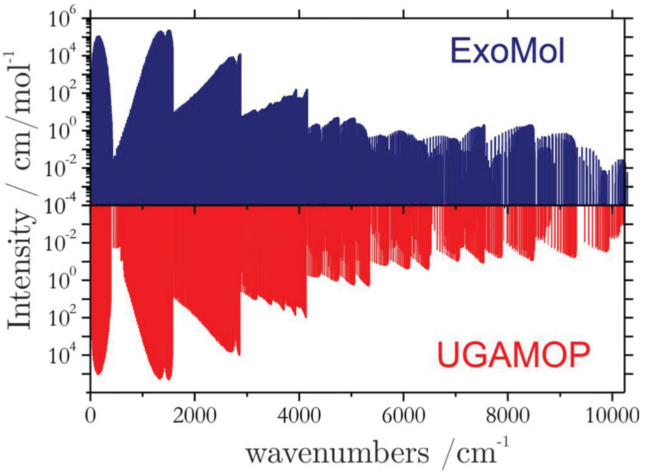

Figure 6. Absorption spectra of MgH at T = 1500 K: ExoMol versus UGAMOP.

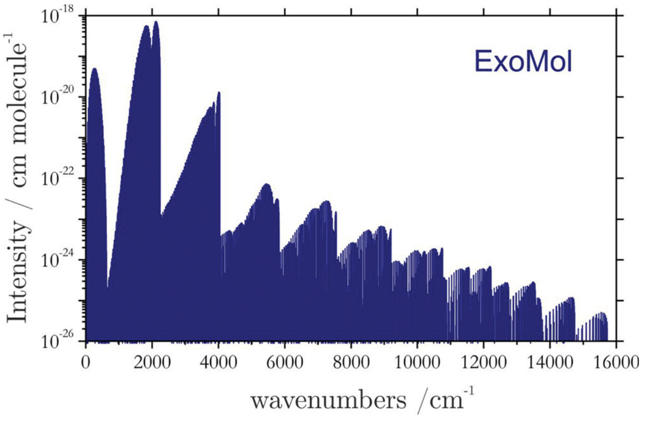

Figure 7. ExoMol absorption spectra of BeH at T = 1500 K.

Irwin (1981) and Sauval & Tatum (1984) one obtains $Z = 659.8$ and 783.2, respectively, to compare with our value $Q/g_s = 811.0$. The factor $g_s = 2$ here is needed to account for the nuclear spin statistics absent in the approach used by Irwin (1981) and Sauval & Tatum (1984) (see discussion in Tennyson & Yurchenko 2012). However, at room temperature even a small difference in $Z(T)$ becomes important. Our value at T = 296 K is 72.8, while Sauval & Tatum (1984) give 65.7. These values are also collected in Table 6 together with corresponding $Z(T)$ obtained for CaH and BeH. Note a striking difference of about 50 per cent for Z(296K) of CaH between our value and that from Sauval & Tatum (1984).

Table 6. BeH, ^{24}MgH and ^{40}CaH partition function, $Z(T)$, expansion parameters for equation (8) and sample partition function values. These values are compared to $Z(T)$ obtained using parameters from UGAMOP and Sauval & Tatum (1984). Note that our and UGAMOP's values are computed using the nuclear statistical factors 8, 2 and 2 for BeH, ^{24}MgH and ^{40}CaH, respectively.

Parameter		BeH	^{24}MgH	^{40}CaH
a_0		−3.69(26)	−4.73(42)	−2.38(36)
a_1		14.63(78)	16.1(12)	9.2(11)
a_2		−17.95(91)	−19.8(14)	−11.5(13)
a_3		11.64(54)	13.01(86)	8.01(75)
a_4		−4.01(18)	−4.61(28)	−2.98(25)
a_5		0.703(30)	0.836(48)	0.564(42)
a_6		−0.0490(21)	−0.0606(33)	−0.0423(29)
		BeH	^{24}MgH	^{40}CaH
g_{ns}		8	2	2
Z(296 K) × g_{ns}	S&T[a]	93.9	129.5	93.9
Z(296 K)	UGAMOP	–	147.8	195.9
Z(296 K)	This work	335.0	145.6	199.9
Z(2000 K) × g_{ns}	S&T[a]	2276.9	1566.4	2276.9
Z(2000 K)	UGAMOP	–	6575.5	2451.7
Z(2000 K)	This work	3019.5	1622.4	2253.5

[a] Sauval & Tatum (1984).

4 CONCLUSIONS

Our potentials are highly accurate for low vibrational levels but there is undoubtedly some loss of accuracy for higher vibrational states given the lack of experimental data to constrain the curves. For BeH, high accuracy should be achieved for all transitions involving states up to v = 11. For MgH, we can be confident of subwavenumber accuracy for $v > 4$ levels as these higher levels can be characterized using electronic transitions. For CaH, it is not possible to test any of the vibrational states higher than $v = 4$ since there is no experimental data.

Line lists for the rotation–vibration transitions within the ground states of the BeH, ^{24}MgH, ^{25}MgH and ^{26}MgH, and ^{40}CaH molecules are presented which should be accurate over an extended temperature range. These line lists were computed using PECs fitted to experimental data and ab initio DMCs obtained at high levels of theory. A complete line list for each of these molecules can be downloaded from the CDS, via ftp://cdsarc.u-strasbg.fr/pub/cats/J/MNRAS/, or http://cdsarc.u-strasbg.fr/viz-bin/qcat?J/MNRAS/. The line lists together with auxiliary data including the potential parameters, dipole moment functions and theoretical energy levels can also be obtained at www.exomol.com.

ACKNOWLEDGMENTS

This work is supported by ERC Advanced Investigator Project 267219. We also thank the present members of the ExoMol team, Ala'a Azzam, Bob Barber, Lorenzo Lodi, Andrei Patrascu, Oleg Polyansky and Clara Silva Sousa, as well as Attila Császár for many helpful discussions on the project and Olga Yurchenko for her help.

REFERENCES

Allard F., Hauschildt P. H., Alexander D. R., Tamanai A., Schweitzer A., 2001, ApJ, 556, 357
Barbuy B., Schiavon R. P., Gregoriohetem J., Singh P. D., Batalha C., 1993, A&AS, 101, 409
Barclay W. L., Anderson M. A., Ziurys L. M., 1993, ApJ, 408, L65
Bell G. D., Herman M., Johns J. W. C., Peck E. R., 1979, Phys. Scr., 20, 609
Bell R. A., Edvardsson B., Gustafsson B., 1985, MNRAS, 212, 497
Berdyugina S. V., Savanov I. S., 1992, Astron. Zh., 69, 829
Berdyugina S. V., Fluri D. M., Ramelli R., Bianda M., Gisler D., Stenflo J. O., 2006, ApJ, 649, L49
Berg L. E., Klynning L., 1974, Phys. Scr., 10, 331
Berg L. E., Klynning L., Martin H., 1976, Opt. Commun., 17, 320
Berg L. E., Ekvall K., Kelly S., 1996, Chem. Phys. Lett., 257, 351
Bernath P. F., Black J. H., Brault J. W., 1985, ApJ, 298, 375
Bonnell J. T., Bell R. A., 1993, MNRAS, 264, 334
Boutalib A., Daudey J., Elmouhtadi M., 1992, Chem. Phys., 167, 111
Brown J. M. et al., 1975, J. Mol. Spectrosc., 55, 500
Burgasser A. J., Kirkpatrick J. D., Liebert J., Burrows A., 2003, ApJ, 594, 510
Carlsund-Levin C., Elander N., Nunez A., Scrinzi A., 2002, Phys. Scr., 65, 306
Chen J., Steimle T. C., 2008, J. Chem. Phys., 128
Chen J. H., Gengler J., Steimle T. C., Brown J. M., 2006, Phys. Rev. A, 73
Clerbaux C., Colin R., 1991, Mol. Phys., 72, 471
Colin R., Dreze C., Steinhauer M., 1983, Canadian J. Phys., 61, 641
Cottrell P. L., 1978, ApJ, 223, 544
Degreef D., Colin R., 1974, J. Mol. Spectrosc., 53, 455
Di Rosa M. D., 2004, European Phys. J. D, 31, 395
Focsa C., Firth S., Bernath P. F., Colin R., 1998, J. Chem. Phys., 109, 5795
Frum C. I., Pickett H. M., 1993, J. Mol. Spectrosc., 159, 329
Frum C. I., Oh J. J., Cohen E. A., Pickett H. M., 1993, ApJ, 408, L61
Gasmi K., Al Tuwirqi R. M., Skowronek S., Telle H. H., Urena A. G., 2003, J. Phys. Chem. A, 107, 10960
Gay P. L., Lambert D. L., 2000, ApJ, 533, 260
Guitou M., Spielfiedel A., Feautrier N., 2010, Chem. Phys. Lett., 488, 145
Herzberg G., 1989, Molecular Spectra and Molecular Structure: I. Spectra of Diatomic Molecules. Krieger Publishing Co., Malabar, FL
Holka F., Urban M., 2006, Chem. Phys. Lett., 426, 252
Huber K. P., Herzberg G., 1979, Molecular Spectra and Molecular Structure IV. Constants of Diatomic Molecules. Van Nostrand Reinhold Company, New York
Hulthèn E., 1927, Phys. Rev., 29, 97
Irwin A., 1981, ApJS, 45, 621
Kaving B., Lindgren B., 1974, Phys. Scr., 10, 81
Kaving B., Lindgren B., 1976, Phys. Scr., 13, 39
Kaving B., Lindgren B., 1981, Phys. Scr., 24, 752
Kaving B., Lindgren B., Ramsay D. A., 1974, Phys. Scr., 10, 73
Kerkines I. S. K., Mavridis A., 2007, J. Phys. Chem. A, 111, 371
Klynning L., Martin H., 1981, J. Phys. B: Atomic Mol. Opt. Phys., 14, L365
Klynning L., Martin H., Nylen P., Royen P., 1982, Phys. Scr., 25, 362
Knowles P. J., Werner H.-J., 1988, Chem. Phys. Lett., 145, 514
Knowles P. J., Hampel C., Werner H.-J., 1993, J. Chem. Phys., 99, 5219
Knowles P. J., Hampel C., Werner H.-J., 2000, J. Chem. Phys., 112, 3106
Koput J., 2011, J. Chem. Phys., 135
Kulaczewski J., Degenhardt D., Kneer F., 1990, A&A, 234, 530
Kurucz R. L., 2011, Canadian J. Phys., 89, 417
Lambert D. L., Mcwilliam A., 1986, ApJ, 304, 436
Lambert D. L., Mallia E. A., Petford A. D., 1971, MNRAS, 154, 265
Le Roy R. J., 2006, dpotfit 1.1: A Computer Program for Fitting Diatomic Molecule Spectral Data to Potential Energy Functions. University of Waterloo Chemical Physics Research Report CP-662R (http://leroy.uwaterloo.ca/programs/)
Le Roy R. J., 2007, level 8.0: A Computer Program for Solving the Radial Schrödinger Equation for Bound and Quasibound Levels. University of Waterloo Chemical Physics Research Report CP-663 (http://leroy.uwaterloo.ca/programs/)
Le Roy R. J., Henderson R. D. E., 2007, Mol. Phys., 105, 663
Le Roy R. J., Appadoo D. R. T., Colin R., Bernath P. F., 2006, J. Mol. Spectrosc., 236, 178
Leininger T., Jeung G., 1995, J. Chem. Phys., 103, 3942
Lemoine B., Demuynck C., Destombes J. L., Davies P. B., 1988, J. Chem. Phys., 89, 673
Leopold K. R., Zink L. R., Evenson K. M., Jennings D. A., Mizushima M., 1986, J. Chem. Phys., 84, 1935
Li X. Z., Paldus J., 1995, J. Chem. Phys., 102, 2013
Liu M., Pauchard T., Sjodin M., Launila O., van der Meulen P., Berg L.-E., 2009, J. Mol. Spectrosc., 257, 105
Lodi L., Tennyson J., 2010, J. Phys.B: Atomic Mol. Opt. Phys., 43, 13301
Martin H., 1984, J. Mol. Spectrosc., 108, 66
Martin H., 1988, J. Chem. Phys., 88, 1797
McGovern M. R., Kirkpatrick J. D., McLean I. S., Burgasser A. J., Prato L., Lowrance P. J., 2004, ApJ, 600, 1020
Mestdagh J. M., de Pujo P., Soep B., Spiegelman F., 2009, Chem. Phys. Lett., 471, 22
Pavlenko Y. V., Harris G. J., Tennyson J., Jones H. R. A., Brown J. M., Hill C., Yakovina L. A., 2008, MNRAS, 386, 1338
Pearse R. W. B., 1929, Proc. R. Soc. Lond. Ser. A, 122, 442
Pereira R., Skowronek S., Urena A. G., Pardo A., Poyato J. M. L., Pardo A. H., 2002, J. Mol. Spectrosc., 212, 17
Petitprez D., Lemoine B., Demuynck C., Destombes J. L., Macke B., 1989, J. Chem. Phys., 91, 4462
Pitarch-Ruiz J., Sanchez-Marin J., Velasco A. M., Martin I., 2008, J. Chem. Phys., 129, 5
Ram R. S., Tereszchuk K., Gordon I. E., Walker K. A., Bernath P. F., 2011, J. Mol. Spectrosc., 266, 86
Reid I. N., Gizis J. E., Cohen J. G., Pahre M. A., Hogg D. W., Cowie L., Hu E., Songaila A., 1997, PASP, 109, 559
Reiners A., Homeier D., Hauschildt P. H., Allard F., 2007, A&A, 473, 245
Sakamoto S., White G. J., Kawaguchi K., Ohishi M., Usuda K. S., Hasegawa T., 1998a, MNRAS, 301, 872
Sakamoto S., White G. J., Kawaguchi K., Ohishi M., Usuda K. S., Hasegawa T., 1998b, MNRAS, 301, 872
Sauval A., Tatum J., 1984, ApJS, 56, 193
Saxon R. P., Kirby K., Liu B., 1978, J. Chem. Phys., 69, 5301
Serrano A., Canuto S., 1998, J. Mol. Struct. (THEOCHEM), 432, 69
Shanmugavel R., Bagare S. P., Rajamanickam N., Balachandra Kumar K., 2008, Serbian Astron. J., 176, 51
Shayesteh A., Bernath P. F., 2011, J. Chem. Phys., 135
Shayesteh A., Tereszchuk K., Bernath P. F., Colin R., 2003, J. Chem. Phys., 118, 1158
Shayesteh A., Appadoo D. R. T., Gordon I., Le Roy R. J., Bernath P. F., 2004a, J. Chem. Phys., 120, 10002
Shayesteh A., Walker K. A., Gordon I., Appadoo D. R. T., Bernath P. F., 2004b, J. Mol. Struct. (THEOCHEM), 695, 23
Shayesteh A., Henderson R. D. E., Le Roy R. J., Bernath P. F., 2007, J. Phys. Chem. A, 111, 12495
Simeckova M., Jacquemart D., Rothman L., Gamache R., Goldman A., 2006, J. Quant. Spectrosc. Radiative Transfer, 98, 130
Skory S., Weck P. F., Stancil P. C., Kirby K., 2003, ApJS, 148, 599
Sotirovski P., 1971, A&A, 14, 319
Steimle T. C., Meyer T. P., Alramadin Y., Bernath P., 1987, J. Mol. Spectrosc., 125, 225
Steimle T. C., Chen J. H., Gengler J., 2004, J. Chem. Phys., 121, 829
Tennyson J., Yurchenko S. N., 2012, MNRAS, doi:10.1111/j.1365-2966.2012.21440.x
Tomkin J., Lambert D. L., 1980, ApJ, 235, 925
Uehara H., 1998, J. Mol. Spectrosc., 192, 417
Urena F. P., Gomez M. F., Gonzalez J. J. L., Rajamanickam N., 2000, Ap&SS, 272, 345
Vidler M., Tennyson J., 2000, J. Chem. Phys., 113, 9766
Wallace L., Hinkle K., Li G., Bernath P., 1999, ApJ, 524, 454
Watson J. K., 2008, J. Mol. Spectrosc., 252, 5
Watson W. W., Weber R. L., 1935, Phys. Rev., 48, 732

Weck P. F., Schweitzer A., Stancil P. C., Hauschildt P. H., Kirby K., 2003a, ApJ, 584, 459
Weck P. F., Schweitzer A., Stancil P. C., Hauschildt P. H., Kirby K., 2003b, ApJ, 582, 1059
Weck P. F., Stancil P. C., Kirby K., 2003c, ApJ, 582, 1263
Weck P. F., Stancil P. C., Kirby K., 2003d, J. Chem. Phys., 118, 9997
Werner H. J. et al., 2010, molpro: A Package of Ab Initio Programs (http://www.molpro.net/)
Wöhl H., 1971, Solar Phys., 16, 362
Woon D. E., Dunning T. H., 1993, J. Chem. Phys., 98, 1358
Woon D. E., Dunning T. H., 1995, J. Chem. Phys., 103, 4572
Wyller A. A., 1961, ApJ, 134, 805
Yong D., Lambert D. L., Ivans I. I., 2003, ApJ, 599, 1357
Zink L. R., Jennings D. A., Evenson K. M., Leopold K. R., 1990, ApJ, 359, L65
Ziurys L. M., Barclay W. L., Anderson M. A., 1993, ApJ, 402, L21

SUPPORTING INFORMATION

Additional Supporting Information may be found in the online version of this paper:

Line lists. The computed line lists for BeH, ^{24}MgH, ^{25}MgH, ^{26}MgH and ^{40}CaH.

This paper has been typeset from a TEX/LATEX file prepared by the author.